Received: 29 December 2015 | Revised: 16 December 2016 | Accepted: 25 January 2017
DOI 10.1111/gec3.12312

WILEY

ARTICLE

An assessment of spatio-temporal variability of land surface temperature using MODIS data: A study of Gujarat state, India

Shashikant Patel[1,2] | **Janak P. Joshi**[2] | **Bindu Bhatt**[2]

[1] Space Applications Centre-ISRO

[2] Department of Geography, Faculty of Science, The Maharaja Sayajirao University of Baroda

Correspondence
Shashikant Patel, Department of Geography, Faculty of Science, The Maharaja Sayajirao University of Baroda, Vadodara, Gujarat, India.
Email: shashikant.gis@gmail.com

Abstract

Land surface temperature (LST) is temperature of the skin surface of land, which can be derived from satellite information or direct measurements. Satellite data provide consistent, continuous, and spatially distributed information on the Earth's surface conditions. The moderate resolution imaging spectro-radiometer instruments installed on the Aqua and Terra Earth observation satellites from NASA, have provided MOD11A2 Product, which contains daytime and nighttime LST in 1 km spatial resolution. Short-term mean (STM) has been calculated using the daytime LST (2002–2011). LST for year 2012, 2013, and 2014 has been analyzed with reference to STM. The study has been carried out for summer season (March to June) that is also called as premonsoon season. Results show that the district of Saurashtra and Ahmadabad experience high LST during summer as compared to districts of South Gujarat. LST analysis is carried out at district and taluka level for entire Gujrat state. Twenty-five districts in Gujarat state contains 179 talukas. Study aims to assess inter and intra-annual and seasonal variability in LST time series data and explores the variation in STM LST and trends in the Gujarat state. The results showed that in 2012 was normal in terms of LST for the summer season, but in the year 2013 experienced above normal or higher LST as compare to STM in almost entire Gujarat during summer season. The analysis showed that the year 2014 summer season also experienced very high LST as compare to the STM. In the year 2013, months of March, April, May, and June, LST is higher than STM in 81, 38, 139, and 43 talukas, respectively.

KEYWORDS

GIS, Gujarat, LST time series, MODIS, spatio-temporal, STM

1 | INTRODUCTION

The science of remote sensing consists of the analysis and interpretation of measurements of electromagnetic radiation that is reflected from or emitted by a target and observed or recorded from a vantage point by an observer or instrument that is not in contact with the target (Mather & Koch, 2011). Also, it is "the science and art of obtaining information about an object, area, or phenomenon through the analysis of data acquired by a device that is not in contact with the object, area or phenomenon under investigation" (Lillesand, Kiefer, & Chipman, 2004). Remote sensing techniques can provide information on the properties of the Earth from local to global scales with a high temporal frequency especially for surface characteristics that have a large spatial heterogeneity, such as land surface temperature (LST) (Wan & Liang, 2009)

Knowledge of the LST is necessary for many environmental studies and management activities of the Earth's surface resources (Li & Becker, 1993). It is one of the key parameters in the physics of land surface processes on regional and global scales, combining the results of all surface–atmosphere interactions and energy fluxes between the atmosphere and the ground (Mannstein, 1987). LST plays an essential role in interactions and energy fluxes at the surface–atmosphere interface (Coll et al., 2005; Sobrino, Kharraz, & Li, 2003). In detail, spatio-temporal variability in LST reveals spatial and temporal changes in the state of the land surface which has been widely implemented in surface energy and water budget estimations (Bastiaanssen, Menenti, Feddes, & Holtslag, 1998; Karnieli et al., 2010; Roerink, Su, & Menenti, 2000). The LST plays an important role in maintain several ecosystem services and also understanding the changes in those services.

Surface temperature has been used in number of applications, including the estimation of evapotranspiration (Hope, 1988; Nemani & Running, 1989), energy balance components (Carlson, Perry, & Schmugge, 1990; Pierce & Congalton, 1988), surface moisture status (Goward, Waring, Dye, & Yang, 1994), and land cover classification (Defries, Hansen, & Townshend, 1995), and the more recent application of LST is used to quantify changes in the physical surface characteristics (Patel, 2006). For the bare soil surface, it is the soil surface temperature, for dense vegetated ground as the canopy surface temperature of the vegetation and for sparse vegetated ground. LST is determined by the temperature of the vegetation canopy, vegetation body and the soil surface (Qin & Karnieli, 1999), and urban heat zones (Joshi & Bhatt, 2012)

From the past studies, it has been observed that temperature trend varies with diverse geographic areas, altitude, and many more climatic parameters. LST, which is retrieved from satellite, remote is captured in the thermal infrared region of the electromagnetic spectrum (Gusso & Fontana, 2005) and is an indicator for measuring the spatio-temporal temperature dynamics and climate change analysis. According to Intergovernmental Panel on Climate Change (2001), increase in greenhouse gas concentrations has influenced the annual mean global temperature by 0.6 ± 0.2 °C since the late 19th century. Various environmental studies and management activities of the Earth surface resources require the knowledge of LST (Li & Becker, 1993). Therefore, the studies using LST is of great importance with respect to the environmental and climate change scenarios.

India is a country with varied topography, which includes high mountains and extensive plateaus and plains, which are in turn responsible for the extraordinary variety of climatic conditions (Patel, Prakash, & Bhatt, 2015).

The remote sensing and geographical information system (GIS) technologies are very useful in natural resource management, ecosystem change detection, environment preservation, and many other significant problems with earth and climate study (Parida et al., 2008). Mapping and monitoring of LST is possible using satellite remote sensing and GIS techniques in spatial and temporal resolution at regional or global scale.

The study aims to assess the spatio-temporal variability of LST using MODIS data for Gujarat. Further, it explores short-term mean (STM) variation in LST and trends.

2 | STUDY AREA AND DATA USED

Gujarat state covers a total geographical area of 196,024 sq. km and accounts for 6.19% of the total area of the country. It is located in the west of India between 20°N to 24°N latitudes and 68°E to 74°E longitudes (Figure 1).

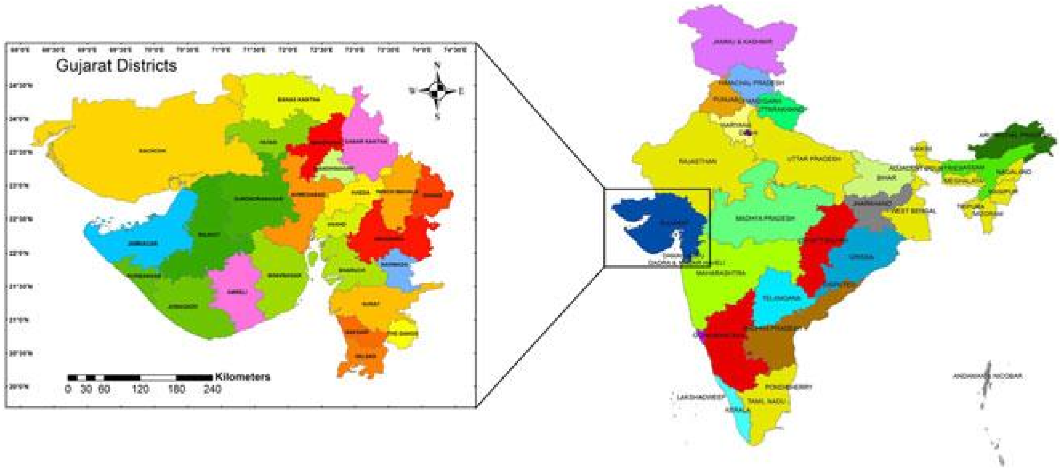

FIGURE 1 Study area Gujarat

In general, Gujarat experience tropical type of climate with three main climatic regions, namely, subhumid, arid, and semiarid spread over different regions of the state. North Gujarat region comprising of Kutch, parts of Banaskantha, Sabarkantha, Mehsana, and North Western part of Saurashtra have arid climate, but the South Gujarat have subhumid climate and in the rest of the state, semi-arid climate. The state is bounded by the Arabian Sea on the west, Pakistan and Rajasthan in the north and northeast, respectively, Madhya Pradesh in the southeast, and Maharashtra in the south. The two deserts, one on the north of Kutch and the other between Kutch and the mainland Gujarat, are saline wastes. It has about 1600 km of coastline, which is about a third of India's total coastline and the longest coastline among all states of India. Gujarat state is subdivided into 25 districts contains 179 talukas as administrative boundaries. District names and their corresponding taluka list is given in Table 1.

3 | METHODOLOGY

The derivation process of the LST initiates from the Preprocessing. This includes subsetting and the removal of spurious data points. These spurious data points encompass pixels affected by clouds and other atmospheric disturbances, which were removed by using the enclosed quality assurance file. Several authors address the importance of such a thoroughly screening of cloud contaminated data points in time series analysis (Chen et al., 2004; Julien & Sobrino, 2010; Julien, Sobrino, & Verhoef, 2006).

The preprocessing included mosaicking and subsetting of all the 8-day images for the duration of 2002–2014 around 552 images of day. In order to calculate the 10-year monthly mean, the MOD11A2 8-day daytime LST tiled product was converted it into ERDAS Imagine file format using batch import tool for further processing. All tiles for the same day have been mosaicked into a single image file, which covers entire Gujarat. Originally product was acquired in sinusoidal projection and it has been used in the same projection as base projection system. Datasets clipped with Gujarat state administrative boundary extracting the study area and annual stack is prepared. In order to retain the temperature values in the actual range, all of the annual stacked images were converted using Equation 1 which converts digital numbers to LST in Kelvin. The monthly accumulated mean has been computed from MODIS11A2, 8-day product and only daytime LST has been taken into consideration.

TABLE 1 Number of districts and respective talukas in Gujarat state, India

S. No.	District	No. of taluka	Taluka name
1	Kachchh	9	Lakhpat, Rapar, Bhachau, Anjar, Bhuj, Nakhatrana, Abdasa, Mandvi, Mundra
2	Banas Kantha	9	Vav, Tharad, Dhanera, Danta, Vadgam, Palanpur, Deesa, Deodar, Kankrej
3	Patan	7	Santalpur, Radhanpur, Sidhpur, Patan, Harij, Sami, Chanasma
4	Mahesana	5	Kheralu, Visnagar, Vijapur, Mahesana, Kadi
5	Sabar Kantha	9	Khedbrahma, Vijaynagar, Idar, Bhiloda, Meghraj, Himatnagar, Prantij, Modasa, Bayad
6	Gandhinagar	2	Kalol, Dehgam
7	Ahmadabad	6	Viramgam, Sanand, Ahmadabad City, Daskroi, Dholka, Dhandhuka
8	Surendranagar	9	Halvad, Dhrangadhra, Dasada, Lakhtar, Wadhwan, Muli, Chotila, Sayla, Limbdi
9	Rajkot	13	Maliya, Morvi, Wankaner, Paddhari, Rajkot, Lodhika, Kotda Sangani, Jasdan, Gondal, Jamkandorna, Upleta, Dhoraji, Jetpur
10	Jamnagar	10	Okhamandal, Khambhalia, Jamnagar, Jodiya, Dhrol, Kalavad, Lalpur, Kalyanpur, Bhanvad, Jamjodhpur
11	Porbandar	3	Porbandar, Ranavav, Kutiyana
12	Junagadh	13	Gir reserved forest, Vanthali, Junagadh, Bhesan, Visavadar, Mendarda, Keshod, Mangrol, Malia, Talala, Patan-Veraval, Kodinar, Una
13	Amreli	9	Kunkavav Vadia, Babra, Lathi, Lilia, Amreli, Dhari, Savar Kundla, Jafrabad, Rajula
14	Bhavnagar	11	Botad, Vallabhipur, Gadhada, Umrala, Bhavnagar, Ghogha, Sihor, Gariadhar, Palitana, Talaja, Mahuva
15	Anand	4	Anand, Petlad, Khambhat, Borsad
16	Kheda	5	Kapadvanj, Mehmedabad, Matar, Nadiad, Thasra
17	Panch Mahals	6	Santrampur, Lunawada, Shehera, Godhra, Kalol, Jambughoda
18	Dohad	4	Dohad, Jhalod, Limkheda, Devgadbaria
19	Vadodara	11	Savli, Vadodara, Vaghodia, Jetpur Pavi, Chhota Udaipur, Nasvadi, Sankheda, Dabhoi, Padra, Karjan, Sinor
20	Narmada	4	Tilakwada, Nandod, Dediapada, Sagbara
21	Bharuch	8	Jambusar, Amod, Vagra, Bharuch, Jhagadia, Anklesvar, Hansot, Valia
22	Surat	13	Olpad, Mangrol, Nizar, Uchchhal, Songadh, Mandvi, Kamrej, Chorasi, Palsana, Bardoli, Vyara, Valod, Mahuva
23	The Dangs	1	The Dangs
24	Navsari	4	Navsari, Gandevi, Chikhli, Bansda
25	Valsad	4	Valsad, Dharampur, Pardi, Umbergaon

Methodology to extract LST values from MOD11A2 product, Equation 1 has been used, where digital numbers or pixel values multiplied by the scale factor 0.02.

$$\textit{Land surface temperature} = \textit{digital number}^{*}0.02. \tag{1}$$

LST pixel values were extracted and calculated for the year 2002 to 2011 for STM. The monthly mean LST is calculated using Equation 2 from MOD11A2 product in the process to evaluate the monthly mean LST; summation of all the 8-day products, which comes in particular month, has been carried out and divided by all nonzeros occurrences.

$$\textit{Monthly mean} = \frac{\sum_i^n \text{8-day LST}}{\textit{Occurance of nonzero values for a month}}. \quad (2)$$

where i = first 8-day LST product in a month and n = last 8-day LST product in a month.

STM has been calculated using Equation 3 where the 10-year monthly mean has been used for calculating STM for particular month. In the process to evaluate the STM for desired month, we have taken a particular month (e.g., March, April, May, and June) from year 2002, 2003, 2004, 2005, 2006, 2007, 2008, 2009, 2010, to 2011. While evaluating the STM, all the nonzero values has been added and divided by number of nonzero observations. The same process has been applied for all months (March, April, May, and June) of summer season.

$$\textit{Monthly short-term mean} = \frac{\sum_1^{10} \text{monthly mean LST}}{\textit{Occurance of nonzero values from } 2000 \textit{ to } 2011}. \quad (3)$$

Initially, all layers have been stacked in image format, and for further analysis in district and taluka level administrative boundaries, the zonal mean statistical analysis has been carried out. The overlay operations using GIS has been performed to get district and taluka level LST values from raster layers.

4 | RESULTS AND DISCUSSION

4.1 | Spatial and temporal distribution of monthly STM MODIS LST (intra- and interannual)

To determine the temporal variation of the surface temperature, LST was plotted at monthly intervals during March to June for the years 2002–2014. The spatial distribution of STM LST in monthly time scale is shown in Figure 2 for entire Gujarat from January to December. Surface temperature patterns derived from this study shows that the STM monthly mean temperature varies spatially as well as temporal. Figure 2a represents the Kutch, north eastern Gujarat (Mehsana, Sabarkantha, Banaskantha, and Panchmahal districts) and the part of south Gujarat (Anand, Surat, Navsari, Valsad, and Bharuch districts) records low surface temperature around 290K to 300K and rest of the Gujarat recording around 302K to 310K. The spatial distribution of surface temperature in the month of February using STM analysis represents the change in temperature ranging from 308K to 314 K in the entire Gujarat except Banaskantha, Kachchh, and partly Kheda and Anand districts, where it is below 300 K.

The surface temperature dynamics study was performed with monthly STM (2002–2011) for whole state and it is observed that the month of March is the start of the summer season. Figure 2c represents the surface temperature in the month of March for STM, where the entire Gujarat records more than 312K except the part of Kachchh, Surat, Navsari, and Bharuch districts. The LST for the month of April and May for STM represents the hottest months of the summer season in the entire Gujarat. Figure 2d and 2e shows the entire Gujarat experienced very high temperature above 318K except the part of Kachchh, Bharuch, Surat, Navsari, Valsad, and part of Banaskantha district. From the study of the summer season for LST, it has been observed that parts of Saurashtra Plateau, namely, Amreli, Bhavnagar, Rajkot, Surendranagar, and Ahmedabad districts experience comparatively very high surface temperature. From the visual interpretation, it has been observed that the surface temperature decreases in the month of June as compare to month of April and May especially in south Gujarat mainly in Surat, Valsad, Navsari, and Bharuch districts, due to southwest monsoon onset (Patel et al., 2015), which is shown in Figure 2f. Figure 2g, 2h, and 2i represents the normal surface temperature with the effect of monsoon rain.

In the monsoon months of July, August, and September, surface temperature ranges from 293K to 310K. Figure 2j represents the surface temperature variation in the month of October, where daytime temperature ranges from 302K to 316K. The month of October is the intermediate month of the monsoon and winter season. Figure 2k and 2l represents the surface temperature for the month of November and December. In the

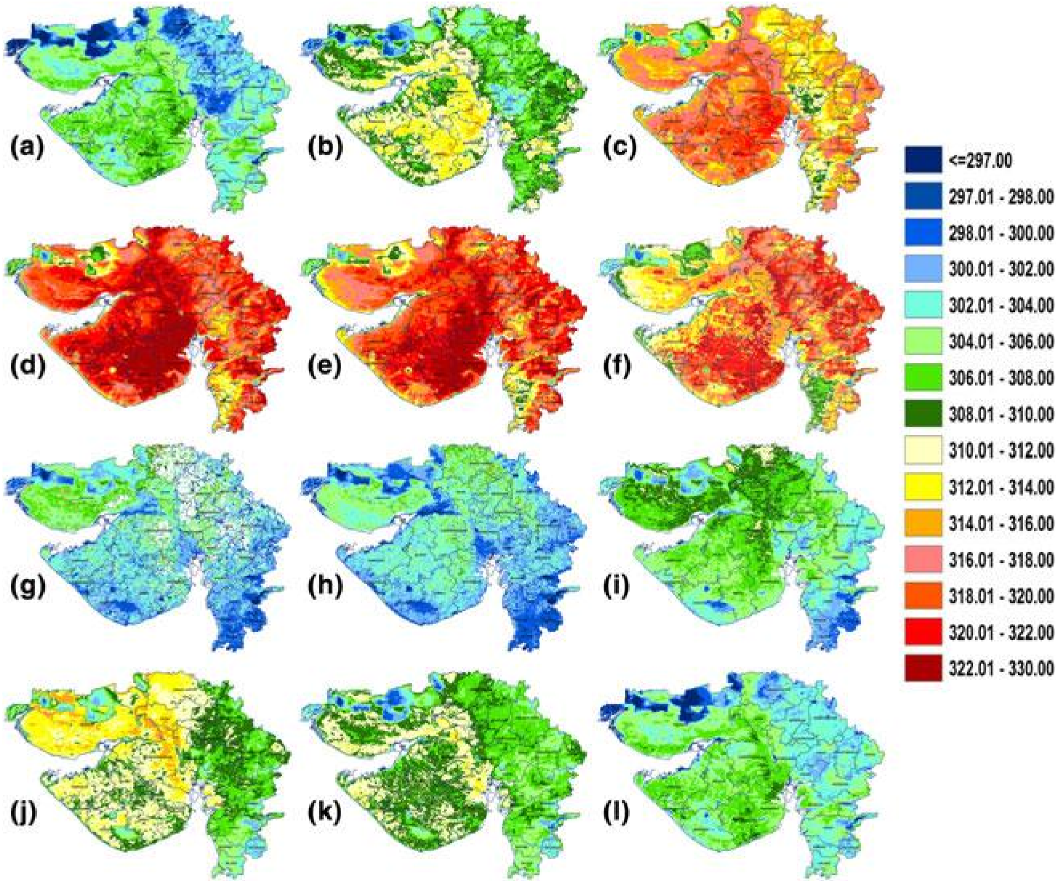

FIGURE 2 Spatial distribution of Short Term Monthly Mean (2002-2011) of LST at 1 km. X 1 km pixel resolution; A-January, B-February, C-March, D-April, E-May, F-June, G-July, H-August, I-September, J-October, K-November, L-December

month of November, it is observed that daytime LST is low as compare to October month, and it ranges from 304K to 308K. The spatial distribution of LST in December shows a low surface temperature ranges from 293K to 308K.

A 10-year (2002–2011) monthly mean LST analysis reveals that the month of March, April, May, and June records very high surface temperature in part of Saurashtra as compare to other months of the year. This is a matter of concern especially for parts of Saurashtra plateau (Surendranagar, Rajkot, Amreli, and Bhavnagar) and Ahmadabad districts. Figure 3 represents taluka level monthly STM (2002–2011) LST for the month of March, April, May, and June, and it is well suited for visual comparison of monthly taluka level LST from year 2012, 2013, to 2014.

4.2 | Spatial and temporal variation of LST during the summer season of 2012–2013

In this section, the LST variations in the summer season for 2012 is assessed from the MODIS satellite, and taluka level monthly mean has been calculated. The monthly mean of LST for the month of April, May, and June has been processed at taluka level for entire Gujarat and represented in Figure 4 (12-A,12-B,12-C, and 12-D). Figure 4 (12-A) illustrates the monthly mean LST of March for the year 2012, and it can be seen that only one or two talukas show LST ranges 318K–320K, and around 20 talukas of Amreli, Rajkot, Jamnagar, Bhavnagar, and Ahmedabad

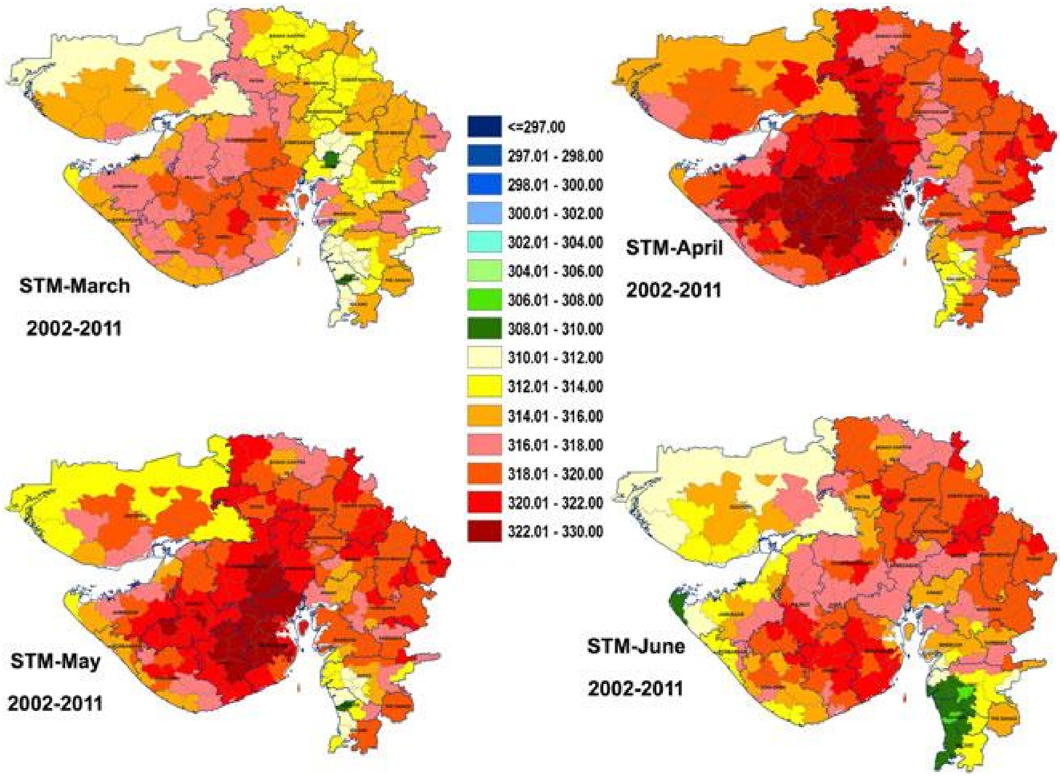

FIGURE 3 Spatial distribution of monthly STM of LST at taluka level for the month of March, April, May, June; summer season

districts show the LST range from 316K to 318K, whereas rest of the Gujarat experiences comparatively low surface temperature below 316K.

Figure 4 (13-A, 13-B, 13-C, and 13-D) illustrates the taluka level LST variations for the year 2013 during the summer season. It has been observed that LST for the month of March, April, May, and June for the year 2013 is comparatively high as compared to 2012 and also for STM. Figure 4 (13-A) represents 81 talukas experiencing above 320K surface temperature and rest of the Gujarat records LST below 320K, a spatial distribution of surface temperature for the month of April for the year 2013 is shown in Figure 4 (13-B). Visual analysis shows that around 38 talukas of six districts, namely, Bhavnagar, Amreli, Junagarh, Rajkot, Surendranagar, and Ahmadabad are experiencing very high surface temperature of above 322K. It is also observed that the month of April 2013 experienced higher LST than the month of April 2012 as well as for April STM.

Figure 4 (13-C) represents the LST variations in month of May for the year 2013, and it shows that almost 50% area of Gujarat is experiencing very high surface temperature of around 322K, which covers parts of Saurashtra plateau, namely, Amreli, Bhavnagar, Rajkot, Jamnagar, Surendranagar, Junagadh, and Ahmadabad. The analysis shows that the month of May2013 is hotter than the month of May 2012 and from the month of May STM.

From the Figure 4 (13-D), it can be analyzed that 43 taluka of Amreli, Junagadh, Bhavnagar, Rajkot, and Jamnagar are experiencing around 322K temperature. Table 2 shows that the number of talukas experienced above normal LST from STM in the year 2013(March, 81; April, 38; May, 139; and June–43). Taluka-wise deviation has been calculated from subtracting the individual month from STM to analyzing year's month, and the results has been compressed in Table 2.

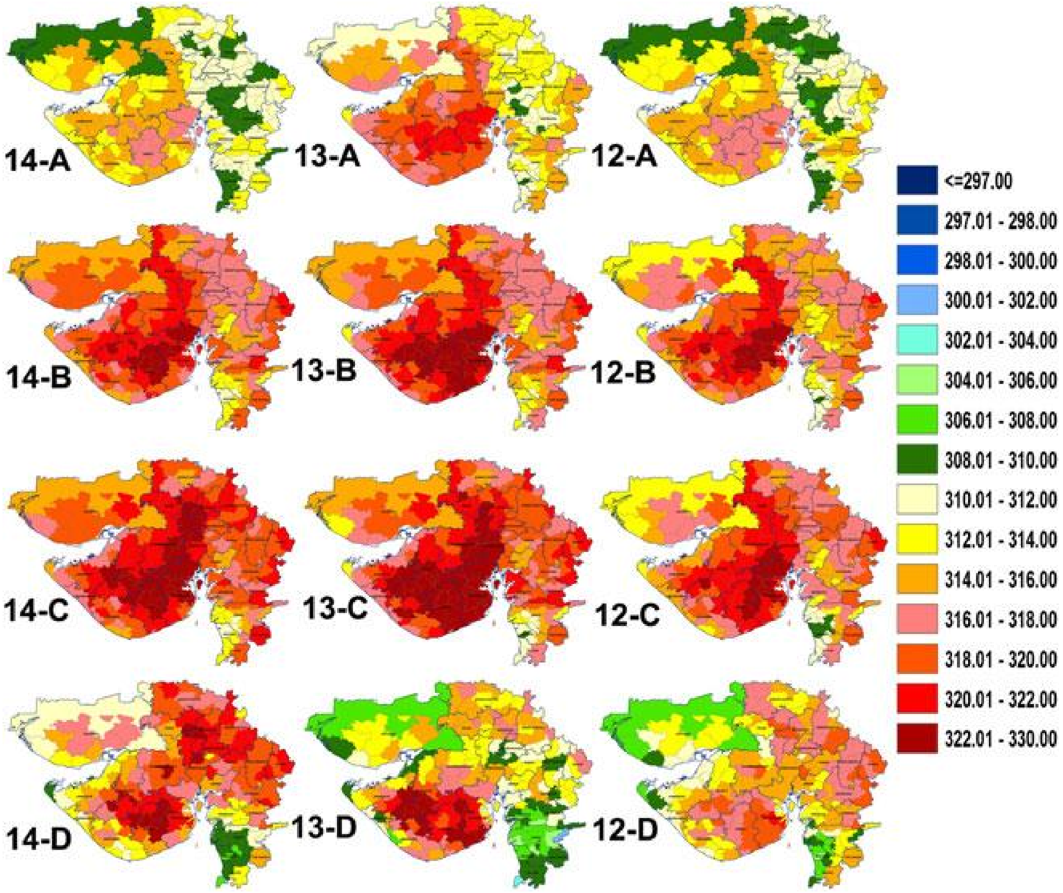

FIGURE 4 Spatial distribution of monthly surface temperature at taluka level for the year 2012, 2013, and 2014 in summer season

4.3 | Temporal and spatial Assessment of LST variations during the summer season of 2014

The spatial distribution of LST for the month of March 2014 is described in Figure 4 (14-A), where the maximum LST is around 318K in around 18 talukas, and the rest of the Gujarat is experiencing below 316K. From Figure 4 (14-A), it can be concluded that the month of March of year 2014 has less temperature as compared to year 2013. Figure 4 (14-B) represents that the 13 talukas of Amreli, Bhavnagar, Rajkot, and Ahmadabad districts records very high surface temperature of more than 322K for the month of April in 2014 while west Gujarat and the central part of the Gujarat

TABLE 2 Number of talukas experienced above normal LST in month of March, April, May, and June as compare to monthly STM (2002–2011)

S. No.	Month	Year 2012	Year 2013	Year 2014
1	March	0	81	4
2	April	0	38	7
3	May	0	139	132
4	June	0	43	102

Note. LST = land surface temperature; STM = short-term mean.

are experiencing around 318K to 322K. And the rest of the parts in state are experiencing surface temperature of 312K to 318K. Spatial variation of LST in the month of May for 2014 is shown in Figure 4 (14-C), where around 30 talukas are experiencing very high surface temperature above 322K in Ahmadabad, Gandhi Nagar, Mahesana, Patan, and parts of Saurashtra plateau, namely, Surendranagar, Bhavnagar, Rajkot, Amreli, Jamnagar and Junagadh; while the rest of the Gujarat also experiences around 316K to 322K except the south part of Gujarat.

Table 2 represents the number of talukas experiencing above normal LST during summer season as compare to the STM (2002–2011), where numbers indicate for the year 2014, four talukas in March, seven talukas in April, 132 talukas in May, and 102 talukas in June experiencing above normal LST out of 179 talukas.

5 | SUMMARY AND CONCLUSIONS

The role of satellite-derived LST over Gujarat at pixel and taluka level has been analyzed using GIS technologies. The monthly mean surface temperature has been calculated from 10-year data and seasonal trend has been analyzed over Gujarat at 1 km pixel as well as taluka level. Figure 5 represents the LST variations of year 2012, 2013, and 2014 over the Gujarat state as compare to STM for the summer season (month of March, April, May, and June). X-axis represent the months of the summer season (1, March; 2, April; 3, May; and 4, June), and Y-axis represents LST in degree Kelvin, whereas the color lines represent different years.

Annual variations in temperature have been analyzed for Gujarat during the period of 2002–2014. The study uses LST analysis based on mean LST for 4 months of summer season concludes that LST may have strong effects on geographical regions. This supports the importance of considering the effect of extremes in studies of historic, contemporary, and future climate change (Parmesan, Root, & Willig, 2000).

Thus, this study gives valuable insights into the complexity of the spatio-temporal variability in LST conditions and contribute to a further understanding of the complex relationship between the spatio-temporal variability of the surface thermal conditions and highlights how these relationships have changed over years. The changing surface temperature is a matter of concerns and needs to be addressed. Major findings in study are spatial variation of LST and LST deviation from STM for the years 2012, 2013, and 2014 at taluka level, where we found that the Saurashtra Plateau and central Gujarat are experiencing very high LST as compare to the rest of Gujarat. Year 2013 and 2014 experienced very high LST in summer season as compare to STM for entire Gujarat. Nonetheless, more validation work needs to be carried out with more integration of satellite data and ground-based measurements over various climatic regions and under different surface conditions in the future.

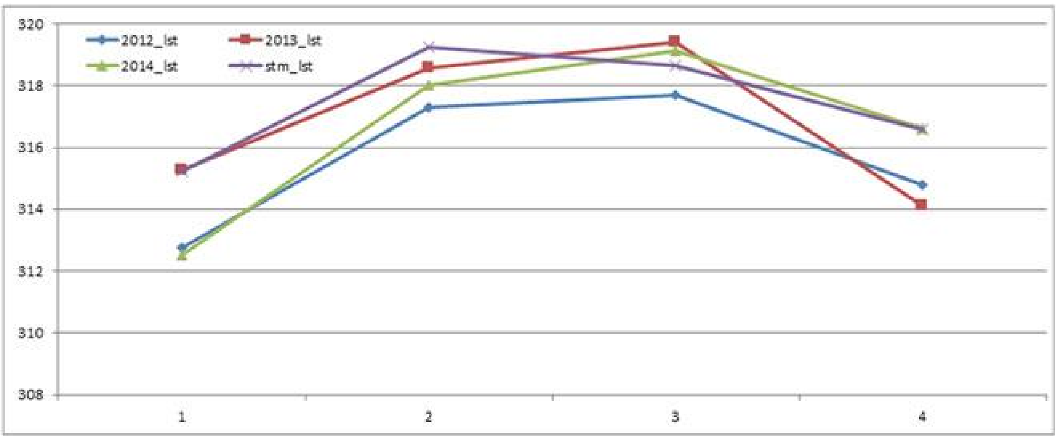

FIGURE 5 Temporal distribution and monthly comparison of LST over Gujarat for the year 2012, 2013, and 2014 in summer season from Short Term Mean (2002-2011)

ACKNOWLEDGEMENTS

The authors would like to thank the Director of Space Applications Centre, Deputy Director of EPSA, Space Applications Centre, and Group Head of VRG, Space Applications Centre for their kind support. The authors also gratefully acknowledge Dr. Markand Oza, Head of CGDD, Space Applications Centre, for his kind support and suggestions.

REFERENCES

Bastiaanssen, W. G. M., Menenti, M., Feddes, R. A., & Holtslag, A. A. M. (1998). A remote sensing surface energy balance algorithm for land (SEBAL). 1. Formulation. *Journal of Hydrology*, *212*(1–4), 198–212. https://doi.org/10.1016/s0022-1694(98)00253-4

Carlson, T. N., Perry, E. M., & Schmugge, T. J. (1990). Remote estimation of soil moisture availability and fractional vegetation cover of agricultural fields. *Agricultural and Forest Meteorology*, *52*, 45–69.

Chen, J., Josson, P., Tamura, M., Gu, Z., Matsushita, B., & Eklundh, L. (2004). 'A simple method for reconstructing a high-quality NDVI Time series dataset based on the Savitzky-Golay filter. *Remote Sensing of Environment*, *91*(3–4), 332–344. https://doi.org/10.1016/j.rse.2004.03.014

Coll, C., Caselles, V., Galve, J. M., Valor, E., Niclos, R., Sanchez, J. M., & Rivas, R. (2005). Ground measurements for the validation of land surface temperatures derived from AATSR and MODIS data. *Remote Sensing of Environment*, *97*(3), 288–300. https://doi.org/10.1016/j.rse.2005.05.007

Defries, R., Hansen, M., & Townshend, J. (1995). Global discrimination of land cover types from metrics derived from the AVHRR pathfinder data. *Remote Sensing of Environment*, *54*(3), 209–222. https://doi.org/10.1016/0034-4257(95)00142-5

Goward, S. N., Waring, R. H., Dye, D. G., & Yang, J. (1994). Ecological Remote sensing at OTTER: Macroscale satellite observation. *Ecological Applications*, *4*(2), 422–343. https://doi.org/10.2307/1941937

Gusso, A., & Fontana, D.C.(2005). Vertical variation survey of the nocturnal air temperature using NOAA/AVHRR satellite data (pp. 173–179). Anais XII symposio Brasileiro desensoriamento Remoto,Goiania, Brasil, 16-21 Abril, INPE, PP.173-179.

Hope, A. S. (1988). Estimation of wheat canopy resistance using combined remotely sensed spectral reflectance and thermal observations. *Remote Sensing Environment*, *24*, 369–383.

IPCC (Intergovernmental Panel on Climate Change) (2001). Climate change 2001: Synthesis report. A contribution of working groups I, II and III to the third assessment report of the Intergovernmental Panel on Climate Change. In R. T. Watson, & the Core Writing Team (Eds.), Cambridge, UK: Cambridge University Press. Retrieved from: www.ipcc.ch/ipccreports/tar/vol4/English/pdf.

Joshi, J. P., & Bhatt, B. (2012). Estimating temporal land surface temperature using remote sensing: A study of vadodara urban area, gujarat. *International Journal of Geology, Earth and Environmental Sciences*, *2*(1), 123–130, ISSN: 2277-2081.

Julien, Y., & Sobrino, J. A. (2010). 'Comparision of cloud-reconstruction method for time series of composite NDVI data. *Remote Sensing of Environment*, *114*, 618–625. https://doi.org/10.1016/j.rse.2009.11.001

Julien, Y., Sobrino, J. A., & Verhoef, W. (2006). Changes in land surface temperature and NDVI values over Europe between 1982 and 1999. *Remote Sensing of Environment*, *103*, 43–55. https://doi.org/10.1016/j.rse.2006.03.011

Karnieli, A., Agam, N., Pinker, R. T., Anderson, M., Imhoff, M. L., Gutman, G. G., … Goldberg, A. (2010). Use of NDVI and land surface temperature for drought assessment: Merits and limitations. *Journal of Climate*, *23*, 618–633. https://doi.org/10.1175/2009JCLI2900.1

Li, Z., & Becker, F. (1993). Feasibility of land surface temperature and emissivity determination from AVHRR data. *Remote Sensing of Environment*, *43*(1), 67–85. https://doi.org/10.1016/0034-4257(93)90065-6

Lillesand, T., Kiefer, R., & Chipman, J. (2004). *Remote sensing and image interpretation* (Fifth ed.). New York: John Wiley & sons.

Mannstein, H. (1987). Surface energy budget, surface temperature and thermal inertia', Remote Sensing Applications in Meteorology and Climatology. In R. A. Vaughan, & D. Reidel (Eds.), (Vol. 201)*NATO ASI Series C: Mathematical and Physical Sciences*. (pp. 391–410). Dordrecht, Netherlands: A Reidel Publishing Co. ISBN: 978-94-010-8225-9.

Mather, P. M., & Koch, M. (2011). *Computer processing of remotely-sensed images—An introduction* (Fourth ed.). Chichester: John Wiley & sons Ltd. ISBN: 978-0470-74239-6.

Nemani, R. R., & Running, S. W. (1989). Estimation of regional surface resistance to ET and TIR AVHRR data. *Journal of Applied Meteorology*, *28*, 267–284. https://doi.org/10.1175/1520-0450(1989)02870276:EORSRT>2.0.co;2

Parida, B. R., Oinam, B., Patel, N. R., Sharma, N., Kandwal, R., & Hazarika, M. K. (2008). Land surface temperature variation in relation to vegetation type using MODIS satellite data in Gujarat state of India. *International Journal of Remote Sensing*, *29*(14), 4219–4235. https://doi.org/10.1080/01431160701871096

Parmesan, C., Root, T. L., & Willig, M. R. (2000). Impacts of extreme weather and climate on terrestrial biota. *Bulletin of the American Meteorological Society*, *81*(3), 443–450. https://doi.org/10.1175/1520-0477(2000)081<0443:IOEWAC>2.3.co;2

Patel, N. R. (2006). Investigating relations between satellite derived land surface parameters and meteorological variables. *Geocarto International*, *21*(3), 47–53. https://doi.org/10.1080/10106040608542392

Patel, S., Prakash, S., & Bhatt, B. (2015). An assessment of Kalpana-1 rainfall product for drought monitoring over India at meteorological sub-divisional scale. *Water International*, *40*(4), 689–702. https://doi.org/10.1080/02508060.2015.1072784

Pierce, L. L., & Congalton, R. G. (1988). A methodology for mapping forest latent heat flux densities using remote sensing. *Remote Sensing of Environment*, *24*(3), 405–418. https://doi.org/10.1016/0034-4257(88)9015-6

Qin, Z., & Karnieli, A. (1999). 'Progress in remote sensing of land surface temperature and ground emissivity using NOAA-AVHRR data. *International Journal of Remote Sensing*, *22*(12), 2367–2393. https://doi.org/10.1080/014311699212074

Roerink, G. J., Su, Z., & Menenti, M. (2000). 'S-SEBI: a simple remote sensing algorithm to estimate the surface energy balance', Physics and Chemistry of the Earth, Part B: Hydrology. *Oceans and Atmosphere*, *25*(2), 147–157. https://doi.org/10.1016/s1464-1909(99)00128-8

Sobrino, J. A., Kharraz, J. E., & Li, Z. L. (2003). Surface temperature and water vapour retrieval from MODIS data. *International Journal of Remote Sensing*, *24*(24), 5161–5182. https://doi.org/10.1080/0143116031000102502

Wan, K., & Liang, S. (2009). Evaluation of ASTER and MODIS land surface temperature and emissivity products using long-term surface longwave radiation observations at SURFRAD sites. *Remote Sensing of Environment*, *113*(7), 1556–1565. https://doi.org/10.1016/j.rse.2009.03.009

How to cite this article: Patel S, Joshi JP, Bhatt B. An assessment of spatio-temporal variability of land surface temperature using MODIS data: A study of Gujarat state, India. *Geography Compass*. 2017;e12312. https://doi.org/10.1111/gec3.12312

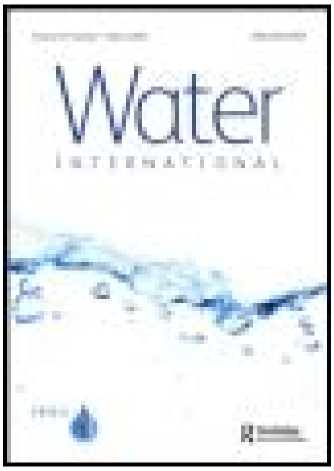

Water International
Publication details, including instructions for authors and subscription information:
http://www.tandfonline.com/loi/rwin20

An assessment of Kalpana-1 rainfall product for drought monitoring over India at meteorological sub-division scale

Shashikant Patel[ab], Satya Prakash[c] & Bindu Bhatt[b]

[a] Space Applications Centre, Indian Space Research Organisation, Ahmedabad, India

[b] Department of Geography, The Maharaja Sayajirao University of Baroda, Vadodara, India

[c] National Centre for Medium Range Weather Forecasting, Earth System Science Organization, Ministry of Earth Sciences, Noida, India

Published online: 27 Jul 2015.

Water International, 2015
http://dx.doi.org/10.1080/02508060.2015.1072784

Routledge
Taylor & Francis Group

TECHNICAL NOTE

An assessment of Kalpana-1 rainfall product for drought monitoring over India at meteorological sub-division scale

Shashikant Patel[a,b], Satya Prakash[c] and Bindu Bhatt[b]

[a]*Space Applications Centre, Indian Space Research Organisation, Ahmedabad, India;* [b]*Department of Geography, The Maharaja Sayajirao University of Baroda, Vadodara, India;* [c]*National Centre for Medium Range Weather Forecasting, Earth System Science Organization, Ministry of Earth Sciences, Noida, India*

(*Received 29 August 2014; accepted 9 July 2015*)

In this study, the potential of Kalpana-1 derived rainfall product is assessed for drought monitoring over India at the meteorological sub-division scale. A preliminary analysis is done for the anomalous south-west monsoon season of 2009 using two drought indices: percent of normal and Standardized Precipitation Index. A considerable difference between these two indices is observed even from the same rainfall data. The severe drought condition over most parts of India during June is not well captured by Kalpana-1 derived rainfall data. Additionally, due to underestimation of orographic rainfall by Kalpana-1 derived product, the meteorological sub-divisions located over these regions showed extreme drought condition throughout the season.

Keywords: monsoon rainfall; rain gauge; satellite-based rainfall estimates; geographical information system; India

Introduction

Drought is considered a natural environmental hazard and has significant adverse impacts on agricultural and socio-economic sectors. Drought is a slowly accumulating regional phenomenon, and its characteristics vary from one climate regime to another (AghaKouchak et al., 2015; Kogan, 1997). Droughts are classified into four categories: meteorological drought (deficit in rainfall); hydrological drought (deficit in water storage); agricultural drought (deficit in soil moisture); and socio-economic drought (deficit in water supply for socio-economic purposes). The first three are referred to as environmental indicators, whereas the last one is considered a water resources indicator.

Meteorological drought is the earliest and the most precise event in the process of occurrence and progression of drought conditions. Low rainfall is the primary driver of the meteorological drought. Ground-based rainfall observations over land areas are accurate but uneven and sparse, especially in unpopulated regions. With the advent of Earth-observation satellites and consistent advancement in rainfall measurement techniques, it is quite reasonable to use satellite-derived rainfall data along with ground observations for drought assessment and hydrological applications as this provides rainfall observations consistently both in space and time (AghaKouchak et al., 2015; AghaKouchak & Nakhjiri, 2012; Kucera et al., 2013; Sorooshian et al., 2011; Tobin & Bennett, 2014). Furthermore, remote sensing and geographical information system (GIS) techniques are now increasingly regarded as useful in drought detection (Jeyaseelan, 2003; Kogan, 1997; Lin & Chen, 2011).

India receives about two-third of its annual rainfall in the south-west monsoon, a four-month period ranging from June to September. This monsoon rainfall has significant socio-economic impacts due to the dependency of Indian agricultural production on monsoon rainfall. Hence, accurate prediction and assessment of droughts and floods are crucial in the Indian context (Bhuiyan, Singh, & Kogan, 2006; Chaudhari & Dadhwal, 2004; Mishra & Liu, 2014; Pai, Sridhar, Guhathakurta, & Hatwar, 2010; Shah & Mishra, 2014). Moreover, drought is likely to be exacerbated in many semi-arid, snow-fed and coastal basins under the current global warming scenario (Damberg & AghaKouchak, 2014; Kogan, Adamenko, & Guo, 2013; Lawler, 2010; Mishra & Singh, 2010; Sheffield, Wood, & Roderick, 2012). Large intra-regional variability of Indian monsoon rainfall and an increasing number of meteorological droughts in recent decades have been reported by Pal and Al-Tabbaa (2011).

To indicate the severity of a drought, various methods and indices have been developed for drought analysis based on different parameters (Alley, 1984; Hao & AghaKouchak, 2013; McKee, Doesken, & Kleist, 1993; Mishra & Singh, 2010; Mu, Zhao, Kimball, McDowell, & Running, 2013). However, parameterization and correlation of these parameters are not always strong and thus there is an eventual disagreement among different drought indices for a particular drought event (Bhuiyan et al., 2006; Chaudhari & Dadhwal, 2004; Khan, Gabriel, & Rana, 2008; Pai et al., 2010). One of the most widely used meteorological drought indices is the Standardized Precipitation Index (SPI) developed by McKee et al. (1993). The advantage of the SPI is that it is applicable to any time scale and is not specific to any location (Agnew, 2000; Chaudhari & Dadhwal, 2004; Patel, Chopra, & Dadhwal, 2007).

Kalpana-1 is the first dedicated meteorological satellite in the Indian National Satellite System (INSAT) series, built by the Indian Space Research Organisation (ISRO). This geostationary satellite was launched by the Polar Satellite Launch Vehicle (PSLV-C4) on 12 September 2002 (Kaila et al., 2002). The satellite carries two payloads, : a three-channel Very High Resolution Radiometer (VHRR) and a Data Relay Transponder for collection and transmission of meteorological, hydrological and oceanographic data from remote data collection platforms. Two rainfall products utilizing Kalpana-1 VHRR data are operational at the India Meteorological Department (IMD; http://www.imd.gov.in) and Meteorological & Oceanographic Satellite Data Archival Centre (http://www.mosdac.gov.in) and are available to users (Gairola, Prakash, Bushair, & Pal, 2014). Among these two rainfall products, the INSAT Multispectral Rainfall Algorithm (IMSRA) takes advantage of the high spatial and temporal coverage of Kalpana-1 and accurate rainfall measurements from the first active microwave precipitation radar (PR) onboard the Tropical Rainfall Measuring Mission (TRMM) satellite for rainfall estimation over the Indian region at 0.25° latitude × 0.25° longitude resolution and 3-hour time interval (Gairola, Mishra, Prakash, & Mahesh, 2010). This rainfall product shows reasonable agreement with other global multi-satellite rainfall products and ground-based observations (Gairola et al., 2014; Prakash, Mahesh, Gairola, & Pal, 2010; Roy, Saha, Fatima, Roy Bhowmik, & Kundu, 2012).

The objective of the present study is to assess the potential of Kalpana-1 derived IMSRA rainfall data for meteorological drought monitoring over India at meteorological sub-division scale. A preliminary analysis is performed for the south-west monsoon of 2009 using two drought indices with the help of GIS, and results are compared with gauge-based rainfall data. According to the IMD report, the 2009 monsoon had the third-largest deficit in rainfall since 1901. India received only 77% of long-period average seasonal rainfall in this year due to prolonged monsoon breaks. We believe that such a study may prove useful for regional and national planners, and for policy makers in drought-proofing and mitigation using space-based observations.

Study area and rainfall data used

India, situated in the heart of South Asia, is the world's seventh-largest country by area and the second-largest by population. India has long coastlines (~7500 km) and two groups of islands besides the mainland: the Andaman and Nicobar Islands in the Bay of Bengal; and Lakshadweep in the Arabian Sea. India is divided into 36 meteorological sub-divisions (Figure 1) based on geographical and climatic conditions. Figure 2 is a map of India showing the varied topography, which includes high mountains and extensive plateaus and plains, which are in turn responsible for the high spatial variability of monsoon rainfall across the country.

Two rainfall data-sets were used in this study. The first was computed from rain-gauge observations and the second was derived exclusively from satellite measurements. The homogeneous monthly rainfall data at meteorological sub-division scale developed by the Indian Institute of Tropical Meteorology for the period 1871–2012 are used as reference data. The network of 306 rain-gauge stations used for the development of this data-set are selected in such a way that each station represents a district having a reliable long-period

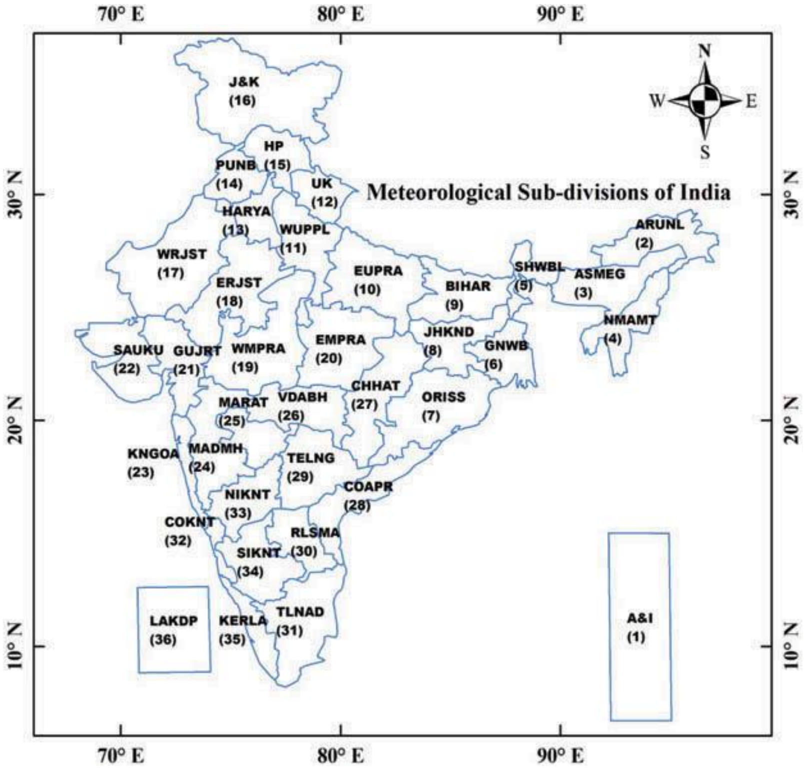

Figure 1. Location map of meteorological sub-divisions in India. The full name of each sub-division is provided in Table 1, and the number in parentheses is the sub-division number.

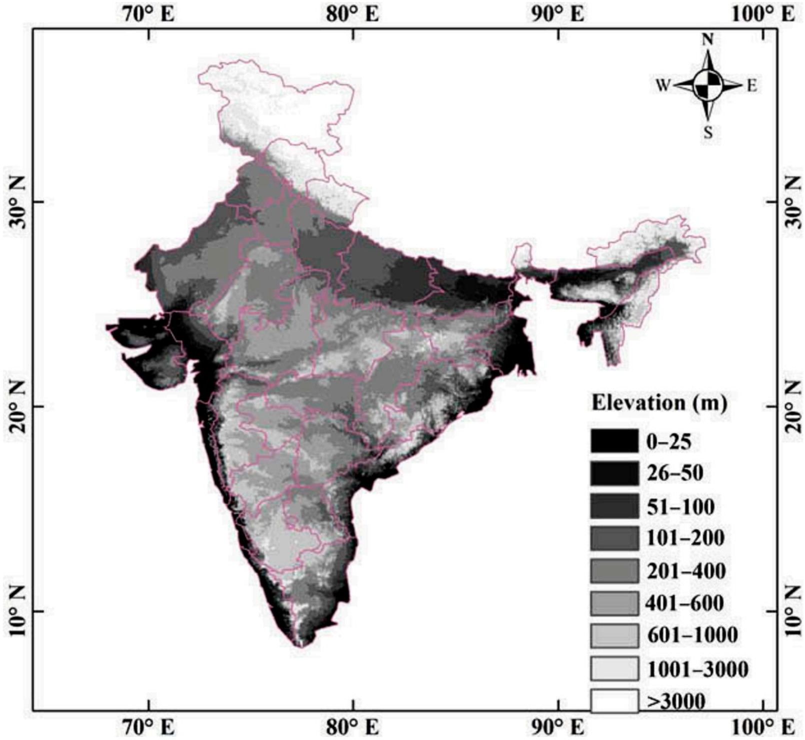

Figure 2. Spatial distribution of topography in India.

record (Parthasarathy, Munot, & Kothawale, 1994). The number of rain gauges in each meteorological sub-division used for the preparation of this data-set is given in Table 1. The hilly regions parallel to the Himalayan range, consisting of four meteorological sub-divisions (Jammu and Kashmir, Himachal Pradesh, Uttaranchal, and Arunachal Pradesh) and the two island sub-divisions (Andaman and Nicobar Islands, and Lakshadweep) were not included in this data-set due to sparse rain-gauge network and low areal representation. The monthly rainfall time series for the other 30 meteorological sub-divisions, which cover about 90% of the country's area, were prepared with an area-weighting method. The gauge-based monthly rainfall data were obtained from the website of the Indian Institute of Tropical Meteorology (http://www.tropmet.res.in).

The other rainfall data-set used in this study is Kalpana-1 derived IMSRA rainfall, which is available at high spatial (0.25° latitude × 0.25° longitude) and temporal (three-hour) resolutions. Kalpana-1 VHRR operates in three wavelength bands: visible, water vapour (WV), and thermal infrared (TIR). In the development of this rainfall estimation algorithm, brightness temperatures in the TIR and WV channels were used for cloud classification. After a suitable cloud classification, a large colocated near-simultaneous database of Kalpana-1 TIR brightness temperature and TRMM-PR rainfall rate was prepared for the development of the rainfall retrieval scheme (Gairola et al., 2010, 2014; Prakash et al., 2010). Kalpana-1 rainfall product based on IMSRA is operational since 2008. This study used IMSRA rainfall data for the south-west monsoon season of 2009 from the MOSDAC website (http://www.mosdac.gov.in). Monthly rainfall was computed by accumulating three-hourly data for a calendar month. Finally, the rainfall

Table 1. Meteorological sub-divisions in India, with abbreviated name (used in Figure 1) and the number of rain-gauge stations in each, used for the development of the homogeneous rainfall data-set.

No.	Name	Short name	No. of stations
1	Andaman and Nicobar Islands	A&I	0
2	Arunachal Pradesh	ARUNL	0
3	Assam and Meghalaya	ASMEG	10
4	Nagaland, Manipur, Mizoram and Tripura	NMAMT	4
5	Sub-Himalayan West Bengal and Sikkim	SHWBL	5
6	Gangetic West Bengal	GNWB	11
7	Orissa	ORISS	13
8	Jharkhand	JHKND	6
9	Bihar	BIHAR	11
10	East Uttar Pradesh	EUPRA	26
11	West Uttar Pradesh	WUPPL	19
12	Uttaranchal	UK	0
13	Haryana, Chandigarh and Delhi	HARYA	12
14	Punjab	PUNJB	10
15	Himachal Pradesh	HP	0
16	Jammu and Kashmir	J&K	0
17	West Rajasthan	WRJST	9
18	East Rajasthan	ERJST	17
19	West Madhya Pradesh	WMPRA	22
20	East Madhya Pradesh	EMPRA	15
21	Gujarat	GUJRT	11
22	Saurashtra, Kutch and Diu	SAUKU	7
23	Konkan and Goa	KNGOA	5
24	Madhya Maharashtra	MADMH	9
25	Marathwada	MARAT	5
26	Vidarbha	VDABH	8
27	Chhattisgarh	CHHAT	6
28	Coastal Andhra Pradesh	COAPR	8
29	Telangana	TELNG	9
30	Rayalaseema	RLSMA	4
31	Tamil Nadu and Pondicherry	TLNAD	15
32	Coastal Karnataka	COKNT	2
33	North Interior Karnataka	NIKNT	6
34	South Interior Karnataka	SIKNT	11
35	Kerala	KERLA	10
36	Lakshadweep	LAKDP	0

at each meteorological sub-division was computed by the use of GIS applications. Recently, Mahesh, Prakash, Gairola, Shah, and Pal (2014) showed the potential of this satellite-based rainfall product for monsoon monitoring over India at meteorological sub-division scale.

Methodology

In order to calculate the mean, standard deviation, and coefficient of variation (CV) of the observed gauge-based rainfall, a separate database was prepared for the each meteorological sub-division for the period 1871–2012. The sub-divisional layer was overlaid on the satellite rainfall and the gauge-based rainfall for the preparation of a sub-division-scale

Table 2. Classification of drought based on percent of normal (PN) and Standardized Precipitation Index (SPI).

Drought class	PN	SPI
Extreme drought	<30%	<–2
Severe drought	<50%	<–1.5
Moderate drought	<75%	<–1
Mild drought	<90%	<0
No drought	>90%	>0

spatial database. The processed results were spatially joined with the base layer, and interactive maps were prepared for better representation using GIS tools. The standard deviation is a measure of dispersion of rainfall from the mean, and the CV is the ratio of the standard deviation to the mean. In the next step, two traditional as well as widely used drought indices, namely percent of normal (PN) and SPI, were calculated for the south-west monsoon of 2009 at each meteorological sub-division using:

$$\mathrm{PN} = (P_i/P) \times 100\% \tag{1}$$

$$\mathrm{SPI} = (P_i - P)/\mathrm{SD} \tag{2}$$

where P_i is the actual precipitation in the current month or season for the ith sub-division, P is the mean precipitation (1871–2012), and SD is the standard deviation of monthly/seasonal precipitation.

PN and SPI are computed from both rainfall data sets for the year 2009. As the IMSRA rainfall product is available since 2008, the mean and SD of rainfall at each meteorological sub-division, computed from the gauge-based rainfall data, are considered for the SPI computation using the satellite-based rainfall data. The classification of meteorological drought using PN and SPI values is presented in the Table 2 in accordance with Pai et al. (2010) and McKee et al. (1993), respectively. PN greater than 90% and SPI greater than zero represent good rainfall activity as compared to the long-term mean and can be used for flood analysis.

Results and discussion

Spatial distributions of mean monsoon rainfall characteristics

In this section, the mean features of the south-west monsoon rainfall are presented at meteorological sub-division scale from gauge-based data for a 142-year period. The mean monsoon rainfall in each meteorological sub-division is shown in Figure 3. Large spatial variability is clearly seen across India. Mean monsoon rainfall varies from 257 mm in west Rajasthan to 2858 mm in coastal Karnataka. The most rainfall occurs along the west coast of India and in north-east India. The least occurs in north-west India and the rain-shadow region of south-east peninsular India. The sub-divisions in the Indo-Gangetic Plain receive a fairly good amount of rainfall (~900 –1200 mm) during this season due to the passage of lows/depressions originating in the Bay of Bengal.

The SD and CV of the monsoon rainfall are presented in Figures 4 and 5, respectively. Large spatial variability in SD, ranging from about 70 mm to 500 mm across the meteorological sub-divisions, is noticed, similar to mean monsoon rainfall. Coastal Karnataka

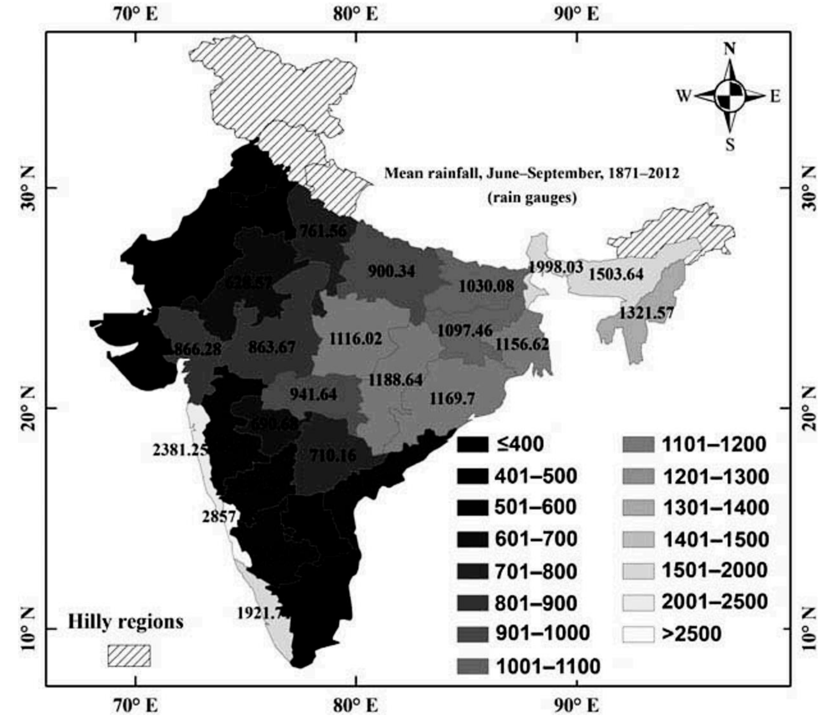

Figure 3. Spatial distribution of mean south-west monsoon rainfall over India at each meteorological sub-division based on rain-gauge data.

(489 mm) and Konkan and Goa (454 mm) show the largest SD, associated with higher mean rainfall, whereas Tamil Nadu shows the least SD (72 mm), associated with lower mean rainfall. The spatial distribution of CV, a normalized measure to assess rainfall variability, is interestingly quite different from the spatial distribution of SD. Fourteen meteorological sub-divisions along the west coast of India, over north-east India, and in the Indo-Gangetic Plain show smaller CV (less than 20%) and are the regions of higher monsoon rainfall activity. Five meteorological sub-divisions in north-west India, receiving rather lower monsoon rainfall, show larger CV, ranging from 30% to 44%, with the maximum in the Saurashtra and Kutch sub-division (44%). The remaining 11 sub-divisions exhibit moderate CV (21–30%). All together, higher mean rainfall regimes generally exhibit larger SD and smaller CV, whereas smaller mean rainfall regimes exhibit smaller SD and larger CV.

Assessment of meteorological drought during monsoon 2009

In this section, the anomalous drought of the 2009 monsoon year is assessed from the satellite and gauge-based data separately at meteorological sub-division scale using PN and SPI methods. The monthly rainfall was 53%, 96%, 73% and 79% of long-period average in June, July, August and September respectively, as per the IMD report. A prolonged hiatus in the advancement of the monsoon between 8 June and 20 June led to

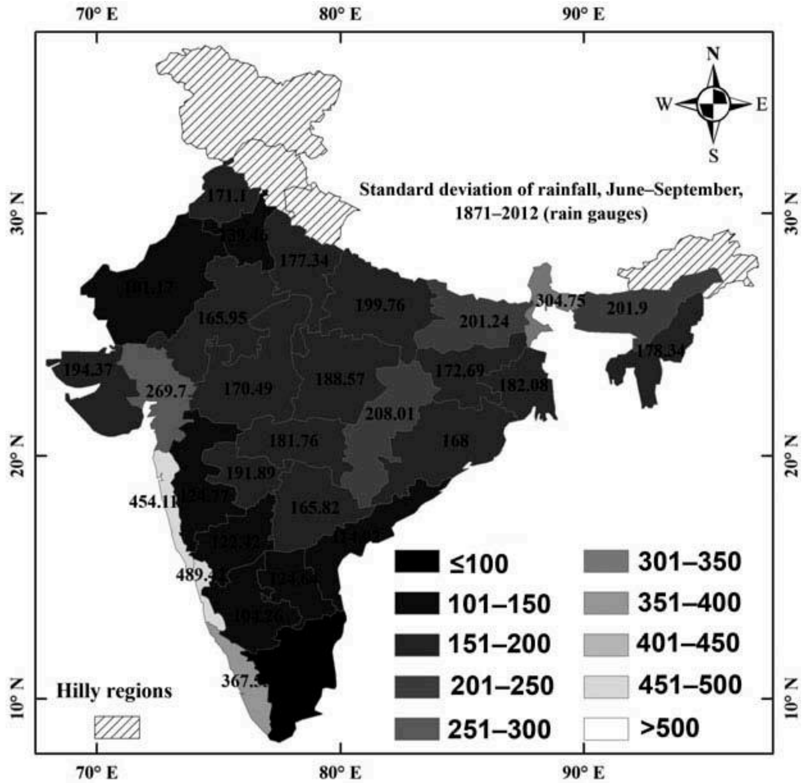

Figure 4. Spatial distribution of standard deviation of south-west monsoon rainfall over India at each meteorological sub-division, based on rain-gauge data.

the unusually low rainfall for June. The PN and SPI are calculated for the rainfall-deficient months of June and August from both types of rainfall data-sets.

Figure 6 illustrates the spatial distributions of PN and SPI from gauge-based and Kalpana-1 rainfall data for the month of June. PN and SPI show notably different classes of drought from the same rainfall data. For example, 6, 11, 9, 2 and 2 meteorological sub-divisions show extreme, severe, moderate, mild and no-drought conditions, respectively, on PN, whereas 1, 5, 14, 10 and 0 sub-divisions show extreme, severe, moderate, mild and no-drought conditions on SPI, using the same gauge-based rainfall data. Sub-divisions in the Indo-Gangetic Plain show severe-to-extreme drought conditions on PN, but SPI shows moderate drought over these regions and mild drought over north-west and south-east peninsular regions. Similarly, 6, 5, 8, 5 and 6 meteorological sub-divisions show extreme, severe, moderate, mild and no-drought conditions, respectively, on PN, whereas 6, 0, 1, 21 and 2 meteorological sub-divisions show extreme, severe, moderate, mild and no drought-conditions, respectively, on SPI using the IMSRA rainfall data. Moreover, a noticeable difference between the drought indices derived from IMSRA and gauge-based rainfall is evident for this month. Mild-to-moderate drought over the three meteorological sub-divisions along the west coast (Kerala, Coastal Karnataka, and Konkan and Goa) on both indices are depicted from the gauge-based rainfall. But these sub-divisions show extreme-drought conditions during this month on both PN and SPI

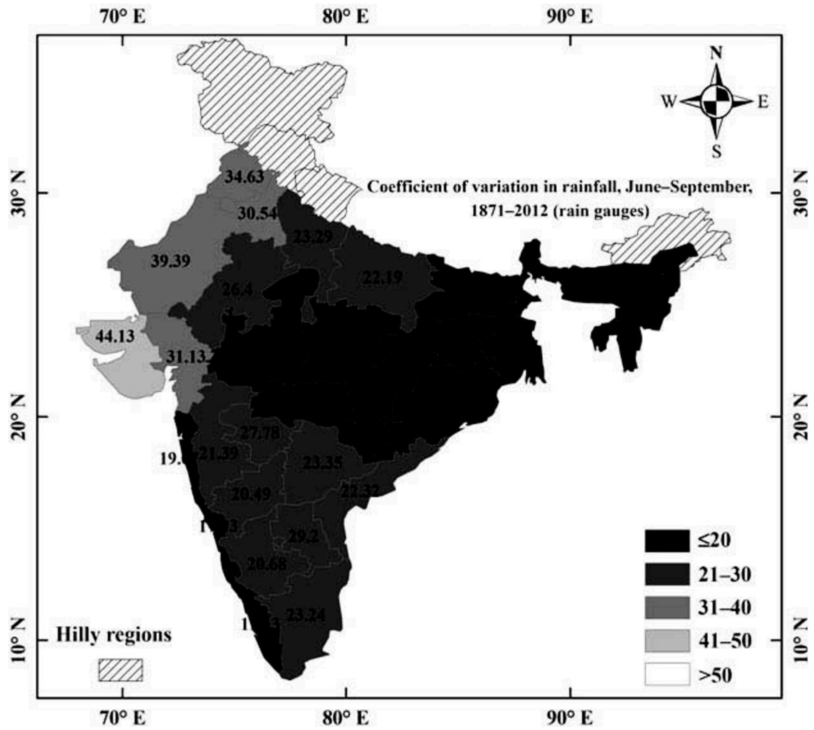

Figure 5. Spatial distribution of coefficient of variation of south-west monsoon rainfall over India at each meteorological sub-division, based on rain-gauge data.

from IMSRA rainfall. This may be because IMSRA underestimates rainfall along the west coast of India due to orography (Gairola et al., 2014; Mahesh et al., 2014; Prakash et al., 2010). There is a large difference between drought classes across most of the meteorological sub-divisions from gauge-based and IMSRA rainfall data using PN. The sub-divisions in the Indo-Gangetic Plain show extreme-to-severe drought conditions on PN using gauge-based rainfall data, whereas these sub-divisions show either mild or no-drought conditions from the IMSRA rainfall data. One of the possible reasons behind this discrepancy is that the Indo-Gangetic Plain receives substantial rainfall from lows and depressions which is considerably over-estimated by IMSRA (Prakash et al., 2010). The agreement between the drought classes from both the rainfall data-sets is notably better in the south-east peninsula and north-west India when the SPI method is used.

The spatial distribution of PN and SPI from gauge-based and Kalpana-1 rainfall data for the month of August is shown in Figure 7. During this month, PN and SPI again show considerable difference in drought classes from the same rainfall data. However, a considerable agreement between the drought classes is noticed using both the indices from gauge-based and IMSRA estimates. From gauge-based data, 0, 6, 9, 5 and 10 meteorological sub-divisions show extreme, severe, moderate, mild and no-drought conditions, respectively, on PN, whereas 3, 5, 8, 4 and 10 sub-divisions show extreme, severe, moderate, mild and no-drought conditions, respectively, from the IMSRA rainfall data. Furthermore, 0, 1, 7, 14 and 8 meteorological sub-divisions show extreme, severe, moderate, mild and no-drought conditions, respectively, on SPI from observed rainfall

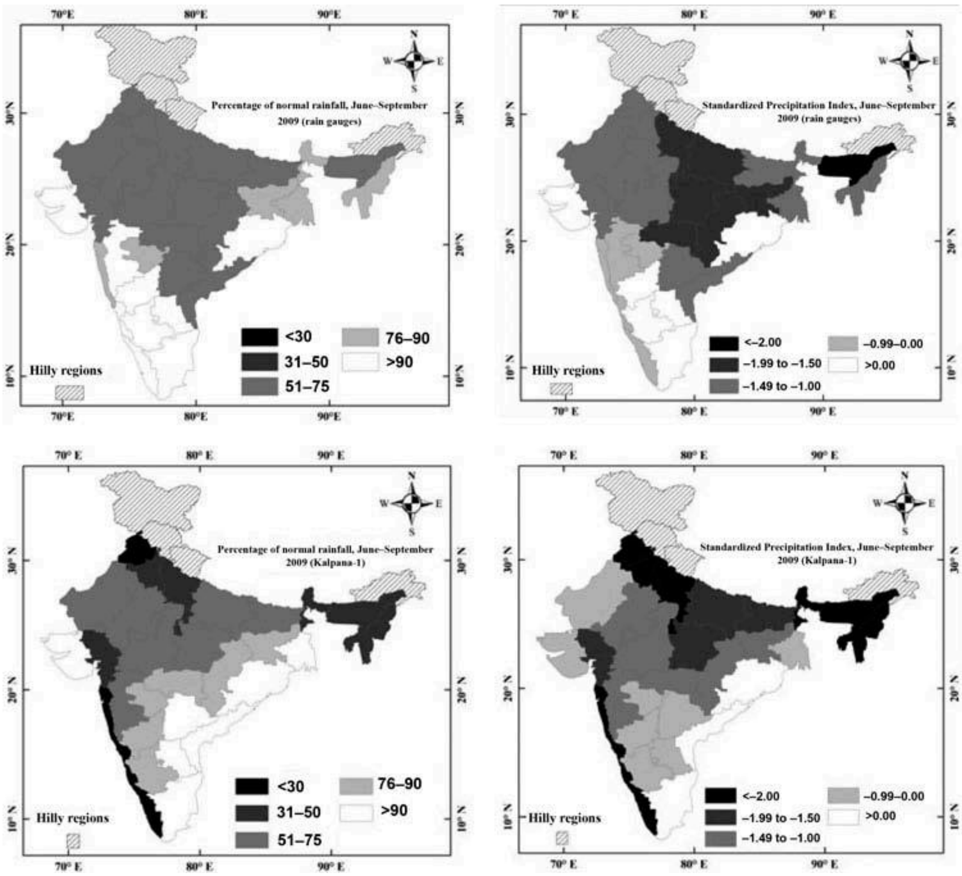

Figure 6. Spatial distribution of PN and SPI from gauge-based and Kalpana-1 derived rainfall data for June 2009 at each meteorological sub-division of India.

data, whereas 2, 3, 7, 10 and 8 sub-divisions show extreme, severe, moderate, mild and no-drought conditions, respectively, from the IMSRA rainfall data. The major difference between observed and satellite-derived rainfall in orographic regions may be the possible cause of the disagreement in drought classes for the sub-divisions along the west coast and north-east India.

The spatial distributions of PN and SPI for the south-west monsoon season (June to September) from observed and Kalpana-1 rainfall data are illustrated in Figure 8. Gauge-based rainfall data depict no severe or extreme drought in India on the PN index, but SPI shows 1 meteorological sub-division in north-east India in extreme drought and 6 in severe drought. Fifteen sub-divisions were under moderate drought using PN, and 12 using SPI, from observed rainfall data. However, IMSRA data depict 4, 6, 7, 6 and 7 sub-divisions from PN under extreme, severe, moderate, mild and no-drought condition, respectively, but 9, 4, 6, 8 and 0 sub-divisions from SPI under extreme, severe, moderate, mild and no-drought condition, respectively. Northern India was affected by drought conditions, whereas the southern peninsular India had no drought conditions, due to normal or above-normal rainfall observed in both data-sets. Three sub-divisions along the west coast were under no or mild drought from gauge-

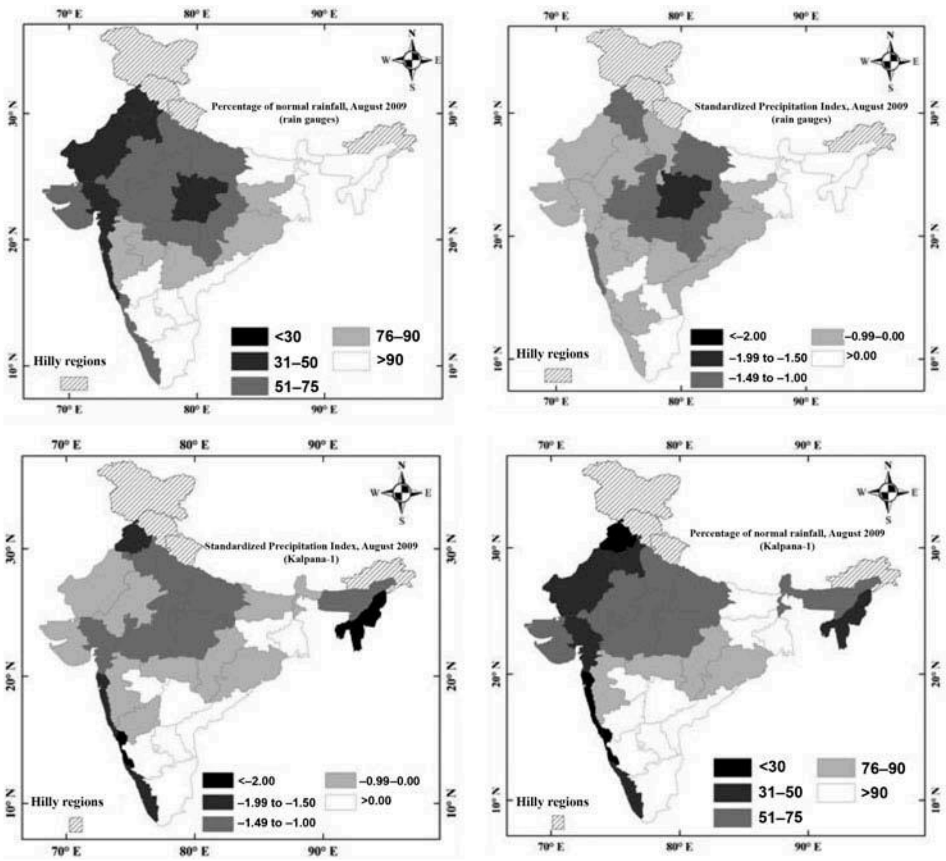

Figure 7. Spatial distribution of PN and SPI from gauge-based and Kalpana-1 derived rainfall data for August 2009 at each meteorological sub-division of India.

based rainfall, whereas the satellite-based rainfall shows extreme drought in these sub-divisions, due to under-estimation of orographic rainfall. Nevertheless, the difference between PN- and SPI-derived drought classes from the same rainfall data is smaller at the seasonal scale. Also, the disagreement between the drought classes from gauge-based and satellite-derived rainfall is smaller. This indicates that IMSRA rainfall data have potential for drought monitoring at seasonal scale except over the orographic regions. However, a suitable bias correction in IMSRA rainfall data is needed before its use for drought monitoring and hydrological applications. Recently, Gairola, Prakash, and Pal (2015) demonstrated that the synergistic use of IMSRA and rain-gauge observations would provide better rainfall estimates over the Indian monsoon region as it benefits from the relative merits of both data sources. Hence, combined Kalpana-1 and rain-gauge rainfall estimates would be better for meteorological drought monitoring over India.

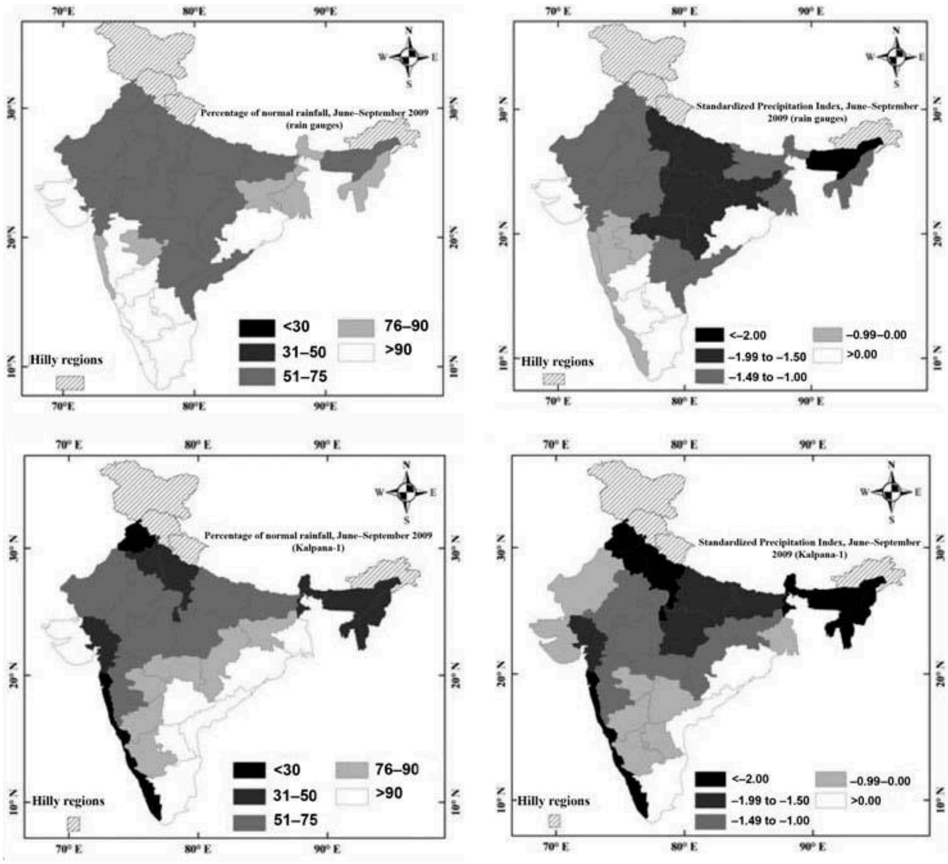

Figure 8. Spatial distribution of PN and SPI from gauge-based and Kalpana-1 derived rainfall data for 2009 seasonal monsoon rainfall at each meteorological sub-division of India.

Conclusion

The role of satellite-derived drought indices is exemplified for drought monitoring in India at meteorological sub-division scale using GIS applications. The anomalous deficit south-west monsoon season of 2009 was selected for this preliminary analysis. Higher CV in the less-rainfall-receiving meteorological sub-divisions and lower CV in the higher-rainfall belts during the monsoon season were evident in the gauge-based rainfall data for a 142-year (1871–2012) period. A notable difference between PN and SPI maps for the same month/season was evident in the same rainfall data-set. There was a notable disagreement between drought classes derived from the gauge-based and IMSRA rainfall data at the monthly scale; the disagreement was much smaller at the seasonal scale. Even though there was difference in the drought classes according to PN versus SPI, the severe drought over India during the month of June was well captured by the gauge-based rainfall data, but IMSRA was unable to display such a drought condition. The meteorological sub-divisions in orographic regions showed continuous extreme drought according to the Kalpana-1 derived rainfall product due to under-estimation of rainfall over these regions. This indicates that IMSRA can be used for drought monitoring over the meteorological sub-divisions of India at seasonal scale, but it has some limitations in orographic regions.

After the huge success of Kalpana-1, the INSAT-3D satellite was launched in July 2013, with a 6-channel VHRR and 19-channel sounder, which added a new dimension to weather and monsoon monitoring through its atmospheric sounding system. The split TIR channels of the INSAT-3D VHRR provide weather observations at a finer spatial scale than Kalpana-1's VHRR. The advanced high-resolution rainfall estimates from the combined use of INSAT-3D and rain-gauge observations will certainly be better for meteorological drought monitoring and other hydrological applications over India.

Acknowledgments

The authors would like to thank the Director, Space Applications Centre, Deputy Director, EPSA, SAC and Group Director, ATDG, SAC for their kind support. Comments and suggestions from the editor, associate editors and anonymous reviewers are greatly appreciated. The Kalpana-1 data from MOSDAC, ISRO, surface rain gauge-derived homogeneous rainfall data from the Indian Institute of Tropical Meteorology, and IMD monsoon report are also thankfully acknowledged.

References

AghaKouchak, A., Farahmand, A., Melton, F. S., Teixeira, J., Anderson, M. C., Wardlow, B. D., & Hain, C. R. (2015). Remote sensing of drought: Progress, challenges and opportunities. *Reviews of Geophysics*, *53*, 452–480. doi:10.1002/2014RG000456

AghaKouchak, A., & Nakhjiri, N. (2012). A near real-time satellite-based global drought climate data record. *Environmental Research Letters*, *7*, 044037. doi:10.1088/1748-9326/7/4/044037

Agnew, C. T. (2000). Using the SPI to identify drought. *Drought Network News*, *12*, 6–12.

Alley, W. M. (1984). The palmer drought severity index: Limitations and assumptions. *Journal of Climate and Applied Meteorology*, *23*, 1100–1109. doi:10.1175/1520-0450(1984)023<1100:TPDSIL>2.0.CO;2

Bhuiyan, C., Singh, R. P., & Kogan, F. N. (2006). Monitoring drought dynamics in the Aravalli region (India) using different indices based on ground and remote sensing data. *International Journal of Applied Earth Observation and Geoinformation*, *8*, 289–302. doi:10.1016/j.jag.2006.03.002.

Chaudhari, K. N., & Dadhwal, V. K. (2004). Assessment of impact of drought-2002 on the production of major kharif and rabi crops using standardized precipitation index. *Journal of Agrometeorology*, *6*, 10–15.

Damberg, L., & AghaKouchak, A. (2014). Global trends and patterns of drought from space. *Theoretical and Applied Climatology*, *117*, 441–448. doi:10.1007/s00704-013-1019-5

Gairola, R. M., Mishra, A., Prakash, S., & Mahesh, C. (2010). Development of INSAT Multi-Spectral Rainfall Algorithm (IMSRA) for monitoring rainfall events over India using KALPANA-IR and TRMM-Precipitation Radar observations. *Scientific Report*, 22 pp., SAC/EPSA/AOSG/INSAT/SR-39/2010.

Gairola, R. M., Prakash, S., Bushair, M. T., & Pal, P. K. (2014). Rainfall estimation from Kalpana-1 satellite data over Indian land and oceanic regions. *Current Science*, *107*, 1275–1282.

Gairola, R. M., Prakash, S., & Pal, P. K. (2015). Improved rainfall estimation over the Indian monsoon region by synergistic use of Kalpana-1 and rain gauge data. *Atmósfera*, *28*, 51–61. doi:10.1016/S0187-6236(15)72159-4

Hao, Z., & AghaKouchak, A. (2013). Multivariate standardized drought index: A parametric multi-index model. *Advances in Water Resources*, *57*, 12–18. doi:10.1016/j.advwatres.2013.03.009.

Jeyaseelan, A. T. (2003). Droughts and floods assessment and monitoring using remote sensing and GIS. In M. V. K. Sivakumar, P. S. Roy, K. Harmsen, & S. K. Saha (Eds.) *Satellite remote sensing and GIS applications in agricultural meteorology*, AGM-8, WMO/TD No. 1182, 291–313. Geneva, Switzerland.

Kaila, V. K., Kiran Kumar, A. S., Sundarmurthy, T. K., Ramkrishnan, S., Prasad, M. V. S., Desai, P. S. … Manikiam, B. (2002). METSAT –A unique mission for weather and climate. *Current Science*, *83*, 1081–1088.

Khan, S., Gabriel, H. F., & Rana, T. (2008). Standard precipitation index to track drought and assess impact of rainfall on watertables in irrigation areas. *Irrigation and Drainage Systems*, *22*, 159–177. doi:10.1007/s10795-008-9049-3.
Kogan, F., Adamenko, T., & Guo, W. (2013). Global and regional drought dynamics in the climate warming era. *Remote Sensing Letters*, *4*, 364–372. doi:10.1080/2150704X.2012.736033.
Kogan, F. N. (1997). Global drought watch from space. *Bulletin of the American Meteorological Society*, *78*, 621–636. doi:10.1175/1520-0477(1997)078<0621:GDWFS>2.0.CO;2
Kucera, P. A., Ebert, E. E., Turk, F. J., Levizzani, V., Kirschbaum, D., Tapiador, F. J. … Borsche, M. (2013). Precipitation from space: Advancing earth system science. *Bulletin of the American Meteorological Society*, *94*, 365–375. doi:10.1175/BAMS-D-11-00171.1
Lawler, A. (2010). The long reach of the monsoon. *Science*, *328*, 566–567. doi:10.1126/science.328.5978.566-b.
Lin, M.-L., & Chen, C.-W. (2011). Using GIS-based spatial geocomputation from remotely sensed data for drought risk-sensitive assessment. *International Journal of Innovative Computing, Information and Control*, *7*, 657–668.
Mahesh, C., Prakash, S., Gairola, R. M., Shah, S., & Pal, P. K. (2014). Meteorological sub-divisional scale rainfall monitoring using Kalpana-1 VHRR measurements. *Geographical Research*, *52*, 328–336. doi:10.1111/1745-5871.12068
McKee, T., Doesken, N., & Kleist, J. (1993). The relationship of drought frequency and duration to time scales. *Eight Conference on Applied Climatology*, Anaheim, CA, pp. 179–184.
Mishra, A., & Liu, S. C. (2014). Changes in precipitation pattern and risk of drought over India in the context of global warming. *Journal of Geophysical Research*: *Atmospheres*, *119*, 7833–7841. doi:10.1002/2014JD021471.
Mishra, A. K., & Singh, V. P. (2010). A review of drought concepts. *Journal of Hydrology*, *391*, 202–216. doi:10.1016/j.jhydrol.2010.07.012.
Mu, Q., Zhao, M., Kimball, J. S., McDowell, N. G., & Running, S. W. (2013). A remotely sensed global terrestrial drought severity index. *Bulletin of the American Meteorological Society*, *94*, 83–98. doi:10.1175/BAMS-D-11-00213.1
Pai, D. S., Sridhar, L., Guhathakurta, P., & Hatwar, H. R. (2010). District wise drought climatology of south west monsoon season over India based on standardized precipitation index (SPI). *NCC Research Report*, RR No. 2/2010.
Pal, I., & Al-Tabbaa, A. (2011). Regional changes of the severities of meteorological droughts and floods in India. *Journal of Geographical Sciences*, *21*, 195–206. doi:10.1007/s11442-011-0838-5
Parthasarathy, B., Munot, A. A., & Kothawale, D. R. (1994). All-India monthly and seasonal rainfall series: 1871-1993. *Theoretical and Applied Climatology*, *49*, 217–224. doi:10.1007/BF00867461
Patel, N. R., Chopra, P., & Dadhwal, V. K. (2007). Analyzing spatial patterns of meteorological drought using standardized precipitation index. *Meteorological Applications*, *14*, 329–336. doi:10.1002/met.33.
Prakash, S., Mahesh, C., Gairola, R. M., & Pal, P. K. (2010). Estimation of Indian summer monsoon rainfall using Kalpana-1 VHRR data and its validation using rain gauge and GPCP data. *Meteorology and Atmospheric Physics*, *110*, 45–57. doi:10.1007/s00703-010-0106-8.
Roy, S. S., Saha, S. B., Fatima, H., Roy Bhowmik, S. K., & Kundu, P. K. (2012). Evaluation of short-period rainfall estimates from Kalpana-1 satellite using MET software. *Journal of Earth System Science*, *121*, 1113–1123. doi:10.1007/s12040-012-0218-2
Shah, R., & Mishra, V. (2014). Evaluation of the reanalysis products for the monsoon season droughts in India. *Journal of Hydrometeorology*, *15*, 1575–1591. doi:10.1175/JHM-D-13-0103.1
Sheffield, J., Wood, E. F., & Roderick, M. L. (2012). Little change in global drought over the past 60 years. *Nature*, *491*, 435–438. doi:10.1038/nature11575.
Sorooshian, S., AghaKouchak, A., Arkin, P., Eylander, J., Foufoula-Georgiou, E., Harmon, R. … Skofronick-Jackson, G. (2011). Advanced concepts on remote sensing of precipitation at multiple scales. *Bulletin of the American Meteorological Society*, *92*, 1353–1357. doi:10.1175/2011BAMS3158.1.
Tobin, K. J., & Bennett, M. E. (2014). Satellite precipitation products and hydrologic applications. *Water International*, *39*, 360–380. doi:10.1080/02508060.2013.870423.